

1
2
3
4
5
6
7
8
9
10
11
12
13
14
15
16
17
18
19
20
21
22
23
24
25
26
27

BIOLOGICAL SCIENCES: Agricultural Sciences

Loss of Photosynthetic Rhythm Thermal Plasticity Under Domestication and Repurposing Drivers of Circadian Clock (DOC) Loci for Adaptive Breeding in Barley

Short title: Repurposing Clock Plasticity Under Domestication

Manas R. Prusty^{*,a}, Eyal Bdolach^{*,a}, Eiji Yamamoto^{*,b}, Jeffrey L. Neyhart^c, Lalit D. Tiwari^a, Klaus Pillen^d, Adi Doron-Feigenbaum^a, Kevin P. Smith^c, and Eyal Fridman^{a,1}

^a Institute of Plant Sciences, Agricultural Research Organization (ARO), The Volcani Center, P. O. Box 6, 5025001, Bet Dagan, Israel

^b Department of Life Sciences Faculty of Agriculture, Meiji University, Japan

^c Department of Agronomy and Plant Genetics, University of Minnesota, St. Paul, MN 55108

^d Institute of Agricultural and Nutritional Sciences, Martin-Luther University Halle-Wittenberg, Halle (Saale), Germany

* These authors equally contributed to this manuscript.

Author for correspondence:

Eyal Fridman

E-mail: fridmane@agri.gov.il, Tel: +972-3-9683901

Keywords: Circadian clock; Domestication; Plasticity; Barley; Genome-wide association studies ; Crop yield; QTL-environment association; Local adaptation

28

29 **Abstract**

30 Circadian clock rhythms are critical to control physiological and development traits,
31 allowing, plants to adapt to changing environments. Here we show that the circadian rhythms
32 of cultivated barley (*Hordeum vulgare*) have slowed and amplitude increased under
33 domestication by comparing with its wild ancestor (*H. spontaneum*). Moreover, we show a
34 significant loss of thermal plasticity during barley evolution for the period and more
35 extensively for amplitude. Our genetic analysis indicates that wild allele at epistatic loci,
36 which mutually condition clock variation and its thermal plasticity in interspecific crosses,
37 are absent in a contemporary barley breeding panel. These epistatic interactions include
38 conditioned effects of Drivers of Circadian (DOC) clock loci on chromosome 3 and 5, which
39 mediate amplitude decrease and period lengthening, respectively, under domestication.
40 Notably, two significant loci, *DOC3.1* and *DOC5.1*, which are not associated with clock
41 diversity in cultivated breeding material, do show pleiotropic effects on flowering time and
42 grain yield at multiple experimental sites across the U.S. in a temperature-dependent manner.
43 We suggest that transition from winter growth of wild barley (*H. spontaneum*) to spring
44 growth of modern cultivars included the loss and repurposing of circadian clock regulators to
45 yield adaptation by mechanisms yet to be clarified.

46

47 **Significance statement**

48 Circadian clock rhythms are crucial factors affecting crop adaptation to changing
49 environments. If faced with increased temperature plants could respond with temperature
50 compensation adaptation and maintain clock rhythms, or they can change period and/or
51 amplitude to adapt. We used a combination of approaches: high-throughput clock analysis
52 under optimal and elevated heat conditions, genome-wide association study (GWAS) with
53 cultivated and wild diversity panels to identify changes under domestication and quantitative
54 trait loci (QTL) that control the clock and its responses, and QTL-environment association
55 for testing environmentally-conditioned effects of these QTL on grain yield and flowering
56 timing across US. Our findings provide insights into changes of circadian rhythms under
57 domestication and genetic tools for plant breeders to develop better-adapted cultivars to
58 changing environments.

59 **Introduction**

60 Growth and metabolism are following rhythms that allow a resonance between
61 environment dynamics, e.g. day and night, and molecular pathways that regulate these
62 biological activities. The core circadian clock is what drives these rhythms, and it is
63 reflecting on the cyclic pattern of different layers or outputs such as photosynthesis, cell
64 division, and metabolism, e.g. starch synthesis and degradation. One hallmark attribute of the
65 circadian clock machinery is that it maintains a relatively stable cycle of about (circa) 24
66 hours (dies)(1). Nevertheless, one emerging question in the study of the circadian clock is to
67 what extent is it robust to environmental changes and does plasticity rather than such
68 robustness or temperature compensation has been selected during natural or artificial
69 evolution, i.e. crop domestication. The change in characteristics of the circadian clock has a
70 major influence on the growth of plants and synchronization with the diurnal cycle is
71 considered a critical adaptive feature of the clock (2, 3). Nevertheless, few studies have
72 utilized naturally occurring variation (4), or made a systematic comparison between wild and
73 cultivated plant material to realize if buffering or flexibility of the circadian clock against
74 increased temperature is more beneficial at the population level. Alternatively, it is not clear
75 yet if selection under domestication and breeding worked against or for plasticity of the
76 clock, and if so, to what characteristic of the clock (period or amplitude, or both)?

77 The core clock in plants composed of three interlocked feedback loops, in which two
78 Myb domain transcription, CIRCADIAN AND CLOCK ASSOCIATED1 (CCA1) and LATE
79 ELONGATED HYPOCOTYL (LHY), are the hubs in these loops. The day-time expression
80 of CCA1 acts to suppress expression in two loops, of TOC1 gene and of the evening complex
81 including ELF4, LUX, GI and ELF3, which in turn work to suppress CCA1 and LHY during
82 the night. In parallel, LHY and CCA1 protein complex are promoting the expression of a
83 family of pseudo-response regulator (PRR) gene family, which in turn close the third loop
84 and suppress LHY and CCA1 to facilitate the day-night cyclic expression of the core clock
85 genes (1). Besides these three interlocked feedbacks loops, the core clock includes additional
86 genes that affect the clock by posttranslational modifications and stabilization of its core
87 components, dependent and independent of the light quality and quantity. The F-box protein
88 ZEITLUPE (ZTL) and clock element GIGANTEA (GI) heterodimerize in the cytosol and
89 hold the later from entering the nucleus and promote flowering (5). Notably, such
90 modifications are rhythmic and also act on gene products in physiological, metabolic and
91 signaling pathways (6), which consider as outputs of the core circadian clock machinery.
92 Photosynthetic activity is one such output that became relevant for the development of non-

93 invasive high throughput measurement of the circadian clock. These remote methods are
94 including prompt and delayed fluorescence (F and DF) from Chl(7–9).

95 Transcript and protein abundance of circadian rhythms have been observed in barley
96 plants as well (10–13). Several studies have reported the diurnal and circadian expression for
97 HvLHY (HvCCA1), HvPPD-H1, HvPRR73, HvPRR59, HvPRR95, HvGI, HvTOC1,
98 HvLUX and HvELF3(14–19). By mutant analysis, three barley clock genes have been well
99 characterized: Ppd-H1, ELF3 and LUX (15, 18–20). The two early maturity mutants, early
100 maturity 8 (*eam8*) and *eam10* barley genes were homologs of the Arabidopsis clock genes
101 ELF3 and LUX1, respectively and mutants plants of both genes showed photoperiod
102 insensitivity and early flowering under long- and short-day conditions in barley (18–20).
103 More recently, analysis of diel and circadian leaf transcriptomes in the cultivar Bowman and
104 derived introgression lines harboring mutations in EARLY FLOWERING 3 (ELF3), LUX
105 ARRHYTHMO 1 (LUX1), and EARLY MATURITY 7 (EAM7) allowed Muller et al. (21)
106 to predict the structure of the barley circadian oscillator and interactions of its components
107 with day-night cues. In fact, some of the critical phenotypes under crop domestication were
108 linked with mutations in the circadian clock genetic network and connected between clock
109 variation to life-history traits relevant for adaptation to agricultural set-up and changing
110 relevant traits (see detailed review (22). In wheat, barley and sorghum PRR-mediated
111 insensitivity to long days was crucial for the transition to the Northern hemisphere, yet it was
112 not implicated in life cycle control but more in the regulation of photoperiod flowering (15,
113 23). At the same time, selection for other clock gene alleles, e.g. *eam8* mutated at the barley
114 HvElf3, which disrupt the dependency of flowering by time-of-the-day light inputs, allowed
115 cultivation further north from the Fertile Crescent, in the shorter growing season of Europe
116 (19). Signature of selection under domestication for clock traits and genes underlying were
117 also reported recently for tomato, in which mutations in *LNK2* and *EIDI*, both involved in
118 light input to the circadian clock, were favored in the cultivated varieties (24).

119 In this study, we utilized our developed SensyPAM high-throughput F-based
120 circadian rhythm measurement platform to estimate and compare the rhythmicity of the
121 clock. We performed this phenotypic analysis on three barley populations with varying
122 proportions of wild vs cultivated allelic diversity. We performed a genome scan, including
123 single and two-dimensional GWAS to describe Drivers of clock (DOC) loci underlying the
124 changes in circadian clock characteristics (their plasticity) between optimal and high
125 temperature environments. Our analysis indicates the significant changes in rhythmicity
126 including period and amplitude, as well as loss of plasticity between the two environments,

127 has occurred under domestication. Furthermore, comparison between genomic architectures
128 underlying clock variation in wild and cultivated populations point to the loss of alleles at
129 specific loci for clock deceleration and for its thermal plasticity. Finally, a QTL–climate
130 association analysis between DOC loci and field phenotype across US indicate the
131 repurposing of plasticity clock QTL for determining grain yield and heading variation thus
132 revealing their potential for adaptive breeding.

133

134 **Results**

135 *Hordeum vulgare* populations with reduced levels of wild *H. spontaneum* DNA diversity show
136 clock deceleration, increased amplitude and reduced thermal plasticity

137 Our initial goal was to compare populations with varying proportions of wild vs cultivated
138 alleles for their thermal circadian clock plasticity. To estimate the rhythms of the clock we
139 used the high throughput F analysis of plants at the 3-4 leaf stage, after these were entrained
140 under long days or short days (14 h of light and 10h of dark and vice versa; see Methods).

141 We estimated the period and amplitude of the clock rhythms from non-photochemical
142 quenching (NPQ) levels measured under continuous light for 3 days. These experiments were
143 conducted under optimal temperature (OT; 22°C) and high temperature (HT; 32°C), which
144 allowed us to calculate the period and amplitude thermal plasticity, i.e. the change of the
145 mean value of the trait for each line between the two environments (HT-OT).

146 Previously we used this SensyPAM platform to extract these clock parameters from a
147 biparental wild barley doubled haploid population (8) however, since we wished to obtain a
148 better representation of the wild gene pool we expanded our analysis. We included
149 representative accessions that were collected in each of the micro-sites of the wild barley
150 infrastructure, Barley1K (B1K), and encompassed all the 51 sites that represent a broad
151 genetic and ecogeographic adaptation (25). On average, the period of the B1K accessions was
152 shortened under HT (HT-OT) by -1.6 hr (Fig. 1a). Nevertheless, there was a varying level of
153 responses to heat between accessions, from relatively robust accessions such as Mt Eitan
154 (B1K-49 site; mean delta of period (dPeriod) of 0.39 h±1.0) to highly plastic ones as Talkid
155 stream (B1K-08 site ; dPeriod of -4.73 h±1.2) (Table S1). Changes in the amplitude of the
156 clock were even more dramatic between the two environments with mean values doubled
157 under HT compared to OT (Fig. 1b; Table S1). As with period, the plasticity in the amplitude
158 also varied between increases of 10% (B1K-37) to more than 400% (B1K-44; Table S1); yet
159 overall there was no overlap between amplitude levels under two environments. Notably, this

160 clock plasticity results are very much alike to those we observed for the bi-parental wild
161 barley doubled haploid population (8).

162 Next, we analyzed the interspecific multiparent barley population HEB-25 that
163 includes 25 wild barley donor accessions into the background of the cultivar Barke (26). In
164 this population, each of the lines is theoretically homozygous for the cultivated genome at
165 71.875% of the sites (26), as compared to none such cultivated diversity in the B1K.
166 Nevertheless, each HEB family is derived from a different *H. spontaneum* accession that
167 originate from the wide barley distribution range including Tibet, Fertile Crescent, and
168 Southern Levant (26). Thermal plasticity of the clock period was similar in direction to that
169 found in the B1K, i.e. a mean dPeriod of -1.52 ± 2.53 ; Fig. 1a; Table S1). However, we
170 observed a much less significant difference in the changes of the clock amplitude between the
171 HEB and B1K collections (Fig. 1b); while the dAmplitude in B1K averaged at +142.6%, that
172 in the HEB lines was half of that (dAmplitude= +72.3%). Since the HEB population is
173 composed of 25 sub-population we partitioned these comparisons to each of the families.
174 This analysis showed that, as between the B1K sites, there was a spectrum of responses
175 between the families with different HID (*H. spontaneum* accessions) donor (Supplementary
176 Fig. S1). For example, while the dAmplitude in the HEB-02 (wild donor is HID004; (26))
177 population was on average +180%, that of lines derived from of HEB-14 (HID144) was
178 almost unchanged (dAmplitude=-4.2%; Supplementary Fig. S1 and S2).

179 Finally, we analyzed the circadian clock responses of elite barley breeding material for the
180 same environmental changes. The US Spring Two-Row Multi-Environment Trial (S2MET)
181 panel is including 232 breeding lines (27), and to the best of our knowledge there was no wild
182 barley material included in its development. A clear difference between the wild and
183 cultivated plant material is the deceleration of the rhythm and increase in the amplitude under
184 optimal temperature in the cultivated barley (Fig. 1a and 1b). While the mean of the wild B1K
185 accessions under OT averaged at 25.5 hr, ranging between 21.04 and 33.1 hr (Table S1), that
186 of the US panel showed a decelerated pace with an average period of 26.1hr under OT. The
187 amplitude of the cultivated material was significantly higher than the wild accessions,
188 showing on average increase of 131% (Table S1; Fig. 1b). These results show clearly that
189 under domestication, as observed for tomato (28), the circadian clock has decelerated, and
190 moreover, under optimal conditions the amplitude has significantly increased. Moreover,
191 unlike the clear plasticity observed in the fully wild (B1K) and interspecific (HEB)
192 populations (Student's t-test; $P < 0.0001$ different than zero), the mean plasticity of the *H.*
193 *vulgare* S2MET lines was not significantly different than zero for period (Student's t-test; P

194 =0.1) and small difference observed for amplitude (Student's t-test; $P=0.01$). These
195 differences between the three gene pools are clearly viewed in the reaction norms between
196 OT and HT (Fig. 1a and 1b). Moreover, analysis for the interactions between the gene pools
197 and the environments support these significant differential responses (ANOVA test;
198 $P<0.0001$) between cultivated, semi-cultivated and wild gene pools (Table S2).

199

200 *Genome wide association study(GWAS) identify genetic network between Drivers of Clock* 201 *(DOC) loci in interspecific population*

202 To identify wild alleles that contribute to these changes in pace and plasticity of the clock
203 between wild and cultivated gene pools we performed a genome scan using clock phenotypes
204 and SNP data available for the HEB-25 population (29). Because the choice of the method
205 used to map the trait plasticity has significant consequence on the results (30), we used the
206 circadian clock phenotype dataset to specify these loci by using three different genetic
207 models (see Methods). Our assumption is that signals that will be repeated in two of the three
208 methods (LMM, MLM and EBL) methods are more reliable and deserve follow-up analysis.
209 We also added to the single point analysis a two-dimensional genome scan to capture
210 possible di-genic epistatic interactions underlying the plasticity.

211 After filtering the SNP data, based on maximum missing genotypes per marker of
212 25%, and minor allele frequency above 3%, we continued the analysis with 3,013 loci (Table
213 S3). Genome scan for the loci affecting trait per-se (under OT or HT), or their plasticity
214 (delta of trait), was initially conducted with a linear mixed model (LMM), which took into
215 consideration the population structure and HEB familial relationships (see Methods). By
216 using a significant threshold determined by Bonferroni correction or BH FDR 0.1 we
217 identified only three significant QTL. One, which we named Driver of Clock 3.1(*DOC3.1*),
218 resides on chromosome 3 (position 29,085,440 -36,987,723; PVE= 4.5 %) and was
219 associated with variation of the amplitude only under HT(Fig. 2a; Table S4a and S4b).
220 Another significant QTL loci, *DOC3.2* (43,840,769-51,509,488) resides on chromosome 3
221 nearby to the *DOC3.1* and the most significant loci in this region is BOPA2_12_31475
222 (position, 51,509,488, LOD = 4.63; PVE= 4.5 %). Notably, the increase in the amplitude
223 under HT for both *DOC3.1* and 3.2 loci was attributed due to the effect of the wild allele for
224 all the markers in these loci (Table S4b, S4c). The third QTL loci named as *DOC5.1*, resides
225 on chromosome 5 (position 605,805,151-608,879,935; and was associated with variation of
226 the period only under OT and the significant marker associated is
227 SCRI_RS_196175(607,080,381, LOD = 4.94 &PVE= 9.8%)(Fig. 2b; Tables S4a and S4b).

228 Also, the shortening of the period by this locus is associated to the wild allele effect for all the
229 markers in this region (Table S4b, S4c). Figure 2c and 2d depict the marker effects of
230 *DOC3.1* and *DOC5.1* on amplitude and period plasticity. While *DOC3.1* is inherited with
231 dominance to the cultivated allele (Fig. 2c), *DOC5.1* seemed to be inherited with dominance
232 to the wild allele (Fig. 2d). It is important to note that only the *DOC3.1*, *DOC3.2* & *DOC5.1*
233 consistently appeared in three of the methods of GWAS i.e LMM, EBL and MLM
234 (Supplementary figure S3). Apart from these, other DOCs appear for the HEB panel such as
235 *DOC5.2* and *DOC6.1* (Table S4), however they are the results from the Tassel MLM model
236 only with a permissive p-values.

237

238 Next, we wished to expand our analysis and look for possible epistatic interactions
239 that may explain the two type of changes in the clock (deceleration under domestication and
240 thermal plasticity). We performed a two-dimensional (2D) GWAS with the results obtained
241 with the HEB population under OT and HT (see Methods). Table S5 summarizes all the
242 significant di-genic interaction that we identified for the different clock traits. Some of the
243 loci that played a role in these interactions were not found in the previous 1D GWAS. We
244 noticed that the interactions between the loci appearing with high additive values are mostly
245 heat-conditioned and act on clock amplitude (Table S5; Fig. 2a; Supplementary Fig. S4). At
246 the same time, conditioning is also found across period (Supplementary Fig. S5) and
247 amplitude, where each member of an interacting pair condition a different trait for the other.
248 For clock amplitude under HT we identified two major interactions between *DOC3.1* or
249 *DOC3.2*, which we identified in 1D analysis, with newly identified loci at of chromosome 5
250 (Table S5). Figure 3 depicts these interactions for both *DOC3.1* and *DOC3.2* with the same
251 locus on chromosome 5. While the interactions of *DOC3.2* were more significant for
252 amplitude and under HT only (Fig. 3a and 3b), those of *DOC3.1* acted reciprocally between
253 the chromosome 3 and 5 on both amplitude and period (Fig. 3c and 3d). This HT-dependent
254 interaction showed that the modulation of clock by *DOC3.1* is conditioned by the allelic
255 combination in chromosome 5 and vice versa. The increase of the amplitude between
256 homozygous for wild and cultivated allele at *DOC3.1* (*DOC3.1*^{Hs/Hs} vs *DOC3.1*^{Hv/Hv}) is
257 conditioned by homozygosity for the wild at the chromosome 5 locus (Fig. 3c). Similarly, but
258 this time for the period, the acceleration of the clock by the chromosome 5 QTL is
259 conditioned by homozygosity at the *DOC3.1* (Fig. 3d). To summarize, these clear digenic
260 interaction (with one locus not identified in 1D GWAS) provides amplitude and period
261 plasticity only for the carriers of the wild alleles at both loci.

262

263 *GWAS for clock diversity in breeding material highlight differential genetic network and lack*
264 *of epistatic interactions*

265 To unravel the genetic network underlying variation in the clock phenotypes, including that
266 underlying thermal plasticity, we repeated the two types of GWAS, i.e. single point and di-
267 genic (1D and 2D), for the S2MET breeding panel using the SensyPAM data we obtained
268 under OT and HT (Table S1). Overall, this genomic architecture included a different set of
269 significant QTL that we associated with clock period, amplitude and their thermal plasticity
270 (Fig. 4). Interestingly, for this breeding panel we did not find any QTL that came consistent
271 with the different models we used. From Tassel MLM, we identified one locus underlying
272 amplitude variation on the telomeric end of chromosome 3 on the, i.e. *DOC3.4*, explaining
273 13.9% and 12.5 % of the amplitude plasticity (delta Amplitude) and its variation under OT,
274 respectively (Fig. 4a, Table S4; see Methods). The most notable locus associated with
275 variation in amplitude of the clock, *DOC7.2b*, explained 14% of the variation for the trait
276 under optimal thermal condition. Finally, we associated one additional QTL, *DOC2.2b*,
277 affecting variation under high temperature on chromosome on chromosome 2. We noticed
278 that loci underlying the period variation, as these affecting amplitudes, in this US panel had
279 higher contribution to the variation. This included *DOC3.3* that explained 10.7% of general
280 period variation under HT, and *DOC2.3* and *DOC5.3* with PVE=8.3% and 8.7%, each is
281 higher from any locus in the HEB population (Table S4).

282 In addition to the interspecific and cultivated populations identifying a different set of
283 DOC QTL (Fig. 2 vs Fig 4; Table S4), the cultivated population exhibited a lack of significant
284 epistatic interactions was, under both temperatures. In any method taken (see Methods) we
285 could not identify in the breeding panel significant di-genic interactions for any of the clock
286 traits (Supplementary Fig. S6 and S7). This is compared to ample amount of significant
287 interactions found for trait per se (amplitude and period) and their plasticity (dAmplitude and
288 dPeriod) in the HEB population (Table S5; Fig. 2).

289

290 *The *DOC3.1* and *DOC5.1* are significantly associated with temperature-dependent effects on*
291 *heading and grain yield*

292 Since we observed a significant loss of plasticity from the wild to the cultivated gene
293 pool and no overlap in loci detected for clock variation between the two populations, we were
294 curious to test if some of the DOC loci identified in HEB population could be associated with
295 other traits in cultivated barley.. The S2MET panel was phenotyped for 14 important traits in

296 39 location-year environments between 2015 and 2017 (27). This allowed us to perform per-
297 trial GWAS for two main fitness traits, i.e. heading date (HEA) and grain yield (GY), using
298 the 5068 high-quantity filtered SNPs (Table S3 and S6). Then, we compared the
299 chromosomal location of the DOC loci identified in the HEB or US panel and checked for
300 co-localization of clock and agronomic trait QTLs. Notably, in these GWAS analyses, SNP
301 associated with heading date were much more consistent across the 39 environments
302 compared with those associated with grain yield implying heading time QTL are more stable
303 than yield. For example, marker S2_429692133 on chromosome 2 (physical position
304 429,692,133) appeared to be significantly linked ($LOD > 3$) with heading date in 16 out of 39
305 (41.02 %) field trials (Table S6). Other heading date markers, that were reproducible across
306 different sites ranged from two to twelve environments whereas the upper limit for yield was
307 (7.6%). To represent the frequency of such stable SNP across different sites, we considered
308 the number of significant SNP and generated a density plot for GY and HEA (Fig. 5a and 5b).
309 In that regard, *DOC3.1* and *DOC5.1* belongs to be more as relatively stable loci for GY, i.e.
310 we identified *DOC3.1* significant effects on GY in up to 3 experimental trials (7%), and for
311 *DOC5.1*, the effect was repeated up to 2 trials depending on the markers we used in the
312 genetic analysis (5.1%; Fig. 5a, Table S7). We could also observe that *DOC5.1*, unlike
313 *DOC3.1*, was also having relatively consistent effect on HEA up to 3 trials (7%) for markers
314 used in the interval (Fig. 5b, Table S6).

315 Moreover, we wished to take a more quantitative approach and examine if the relative
316 level of genetic association, i.e. its significance, with GY and HEA are conditioned by the
317 environmental variation, therefore suggesting that they are involved in local adaptation. To
318 test the possible relationship between environmental gradients and effect of the DOC loci, we
319 correlated the per-trial GWAS $-\log_{10}(p)$ values of the two traits (HEA and GY) for *DOC3.1*
320 and *DOC5.1* with the environmental covariates (e.g. temperature and rainfall) recorded during
321 these experiments. Also, we made these correlations between GWAS $-\log_{10}(p)$ values and the
322 calculated variation of these environmental covariates, e.g. the coefficient of variation (CV)
323 for minimal daily (night) temperature (Tmin) that represent the stability of the environmental
324 conditions (see Methods). Finally, we made these correlations with regard to the mean
325 normalized flowering time in each location to ask if the effect of the DOC locus is more or
326 less effective depending on the stability of heading. The full details of the correlation
327 coefficient between the per-trial GWAS $-\log_{10}(p)$ values and the different environmental
328 covariates are depicted in Table S8. Generally, we found a significant negative correlation
329 between $-\log_{10}(p)$ values of *DOC3.1* markers for grain yield and the mean normalized

330 heading date of the whole panel on trial ($r = -0.37$, $P=0.03$; Fig. 5c). We found similar
331 correlation between HEA stability of the trial and the significance of the *DOC5.1* effects on
332 grain yield ($r = -0.35$, $P=0.04$; Fig. 5c). These results suggest that the more variable was the
333 flowering between lines the higher was the effect of the *DOC3.1* or *DOC5.1* on grain GY
334 variation.

335 When we tested the correlations between the environmental covariates and the effect
336 of the two loci on GY or HEA we found a difference between the two loci. For *DOC3.1*, we
337 could identify a significant negative correlation ($r=-0.35$, $P=0.04$) between T_{min} in the site of
338 experiment and the specific *DOC3.1* GWAS $-\log_{10}(p)$ for GY (Fig. 5e). On the other hand,
339 the correlation between GWAS $-\log_{10}(P)$ of GY with temperature or other environmental
340 gradients in sites were marginal. For example, the highest correlation of $r=0.3$ ($P=0.055$) was
341 observed between the range of maximal daily temperature (maxT_{mean}) and $-\log_{10}(p)$ of
342 GWAS for GY (Table S8; Fig. 5f). Nevertheless, the correlations between environmental
343 covariates in experimental site with the GWAS $-\log_{10}(p)$ values for *DOC5.1* on HEA were
344 much more significant and abundant. Moreover, these correlations appear both for the means
345 per se, as well as for the CV of the temperatures and precipitation values. We found a strong
346 positive correlation between per-site $-\log_{10}(p)$ for HEA with T_{max} ($r=0.47$, $P=0.0037$; Fig.
347 5g), as well as significant correlation with CV T_{max} ($r=0.5$, $P=0.0017$; Fig. 5h). These results
348 indicate higher and/or unstable temperatures during growth period are associated with the
349 effect of the *DOC5.1* on the flowering time variation.

350 .

351 Finally, we made these quantitative correlations between environmental covariates
352 and genetic significance for the DOC loci identified in the US S2MET panel (Fig. 4; Table
353 S4a). It is interesting to note that unlike the environmental-QTL correlation for effects on GY
354 we identified for the wild allele of *DOC3.1*, we could not find any such relationship ($P>0.05$)
355 for any of the DOC loci identified in the GWAS of this material. These QTL-environment
356 correlations could only be found for the effects of *DOC3.4* and *DOC5.3* on HEA variation
357 (Table S8).

358 **Discussion**

360 *The nature of circadian clock changes under domestication*

361 A clear difference between wild and modern breeding material is that wild accessions
362 accelerate their rhythmicity and increase their amplitude oscillation under heat, while the
363 cultivated genotypes are much less responsive and overall maintain a similar peripheral clock

364 (Fig. 1). In the current study we used a high throughput readout of non-photochemical
365 quenching (NPQ) to obtain measures of clock rhythmicity (period and amplitude).
366 Previously, Dakhiya et al. (7) showed that NPQ oscillation gives a fairly good proximation
367 for the clock rhythms by comparing clock genes to F-based readouts in Fytoscope, mainly by
368 using Arabidopsis mutants, i.e. *cca1* and *lhy*. Nevertheless, we showed that genetic changes
369 in these rhythms are not always correspondent to the responses of the core clock genes, e.g.
370 CCA1, and that these probably correspond better to peripheral rhythms such as
371 photosynthesis. For example, the effect of the wild barley allele at *frp2.2* locus accelerated
372 the clock under heat yet examination of CCA1 and TOC1 temporal expression did not find
373 significant effect of this locus on this core clock gene (8). Nevertheless, despite the fact that
374 as wild barley was faced with a more extreme environment compared to contemporary
375 breeding material, there seems to be an advantage for plasticity of these rhythms, either
376 directly affected by the core clock or in its transduction to peripheral activities. Accelerating
377 the clock suggest that in a similar manner to seasonal escape mechanism, where cereal that
378 flower earlier avoid detrimental conditions for growth and reproduction phase(31), higher
379 daily pace may support avoidance of physiological activities in more stressful periods of the
380 day. . Further detailed physiological and molecular analysis of nearly-isogenic lines for the
381 DOC identified in this study, including the differential transcriptome and metabolome
382 changes, should unravel the main pathways that will explain this accelerating strategy and its
383 possible benefits for fitness.

384

385 *Genetic diversity underlying loss of clock plasticity under domestication*

386 The type of genetic material investigated in this study, as well as other comparisons between
387 genotypic and phenotypic diversity under domestication(32–34), consider nuclear genome
388 diversity that had obviously undergone a bottleneck (35). Moreover, recent studies are
389 attempting to identify signatures of selection by identifying genetic sweeps across these
390 nuclear genomes between wild and cultivated panels (36, 37). Interestingly, few of the loci
391 we identified in this study overlap with some of the resequenced genes reported under
392 selective sweep between wild and cultivated barley (38). This is including overlapping of the
393 *DOC3.2* loci marker SCRI_RS_141171 (43,840,769) with that of BOPA2_12_30924, which
394 is located on chromosome 3 631,804,839. Pankin et al.(38)found that the gene
395 HORVU3Hr1G090440.4 spanning 631,804,086-631,808069 is under selection. However,
396 since at least one of the major DOC loci we identified in this study, *DOC3.1*, has not been
397 included in the list of candidate domestication genes, it is still an open question as to loss of

398 these DOC loci resulted in a signature of selection. Combining our top-down QTL approach
399 with such bottom-up analysis could be instrumental in finding the causal variation underlying
400 functionality of genes and their selective advantage.

401 Furthermore, with regard to the circadian clock variation and its change under
402 domestication, as we report in this study (Fig. 1), there may be additional overlooked source
403 of diversity that went through a genetic sweep and which has affected the loss of plasticity in
404 the cultivated breeding material. Previously, our study of reciprocal doubled haploids within
405 wild barley have shown a significant difference in the thermal response of the circadian clock
406 that we could link with plasmotype diversity (8). This variation corresponded to 6 non-
407 synonymous mutations between the founders of the populations. This suggests that in the
408 search of variation on the clock, we should consider and design experiments that will
409 examine the direct links between plasmotype diversity and circadian clock variation under
410 different environments, as well as cytonuclear interactions. Such designs should also consider
411 the fact that there is a biologically relevant interaction between the chloroplast and nuclear
412 genomes, i.e. retrograde signaling(39), and that effects of nuclear genes on the clock and its
413 output could be conditioned by protein or RNA partners encoded in the organelle. In fact, we
414 recently generated a relevant cytoplasmic multi parent population (CMPP) that includes
415 introduction of ten wild barley cytoplasm into the background of the cultivated barley(40).
416 This new fully-homozygous infrastructure will allow us to explore these cytonuclear
417 interactions for different phenotypic layers including circadian clock and agronomic traits in
418 multiple sites, and to investigate in depth how such pleiotropy is maintained or lost in
419 accordance with environmental changes.

420

421 *QTL-environment association for detecting local adaptation*

422 Recently, Wadgymer et al. (41) proposed a framework for evaluating the nature of local
423 adaptation including distinguishing between genetic tradeoffs and conditional neutrality of
424 QTL involved in local adaptation. They, and others (42) proposed that loci that have effects
425 on fitness in one environment, but not in alternative environments (i.e., conditional
426 neutrality), appear to be more common. From an agricultural point of view, and obviously for
427 the same reason of local adaptation, crop breeding is done in the target area to allow better
428 relevance of the material. Indeed, same group took this approach and tested a panel of
429 switchgrass and showed that adaptive trait variation has beneficial effects in some geographic
430 regions while conferring little or no detectable cost in other parts of the geographic range
431 (43). Similarly, here we demonstrate that among the significantly associated loci the

432 percentage of markers repeated in more than several sites/years is low for GY and much more
433 for HEA (Fig. 5a and 5b). This could be because GY is a complex trait with relatively low
434 heritability that influence from several other traits(44). Nevertheless, the markers found for
435 clock rhythmicity (DOCs) are found significant for HEA and GY in more trials than other
436 markers, suggesting that they are involved in local adaptation. Moreover, we also provide an
437 alternative quantitative approach to test the level of local adaptation with regard to the
438 environmental agents involved. This is simply done by performing per-trial GWAS to obtain
439 the significance (P value) of the SNPs and then perform correlation, or other similar
440 association test, to examine relationship of significance with environmental co-variates. This
441 approach is different than counting the frequency of single nucleotide polymorphisms (SNPs)
442 associated with fitness and how it co-varied with climate across the range of experiments
443 conducted (Fournier-Level et al. 2013).

444

445 *The adaptive value of plasticity vs robustness under domestication and its molecular basis*

446 In a previous study, we showed that within the wild barley populations there is a
447 standing variation for the circadian clock plasticity and that that it varies between accessions
448 adapted to different niches. For example, the B1K-09-07 that served as a parent of the
449 ASHER DH population showed significant shortening of the clock rhythm (by more than 3
450 hr; (8)). This is compared to relative robust clock of B1K-50-04, an accession from the colder
451 Northern part of the B1K collection (25), for which the period shortened slightly by one hour.
452 This, and the fact that a significant relationship between temperature at the site of collection
453 and the clock period was found indicated the adaptive value of the clock to changing
454 environment in the wild(7). But how would that be relevant in agriculture, and why do we
455 observe loss of such plasticity, as exemplified by overall lesser response for both period and
456 amplitude (Fig. 1), and also by loss of significant plasticity QTL such as *DOC3.1*? One
457 obvious reason might be that modern cultivars were bred in a more stable environment than
458 their wild ancestors, and more specifically, more homogeneity in sites in the different sites of
459 cultivation vs growth of wild populations in wide adaptive niche (25).

460 Vis-à-vis adaptation under domestication for barley and lack of environmental
461 responsiveness involved, it was shown previously that misexpression of barley ortholog for
462 the Arabidopsis circadian-clock gene *ELF3* of circadian clock gene in the *eam* mutants (19).
463 This mutation allowed early-flowering day-neutral phenotype with rapid flowering under
464 either short or long day (45). This may suggest that under cultivation loss or change of
465 circadian clock functions such as light responses have been favored, e.g. deletion and

466 mutations in the EID and LNK2 genes in cultivated tomato found to be responsible for the
467 clock deceleration (24). Since a direct link between allelic changes from wild to the
468 cultivated tomato for yield has not been shown yet, but only that of growth (24), it is still
469 remains to be studied what is the adaptive value of these mutations. Besides, are loss of
470 function for clock genes is typical to these changes under domestication as reported so far?
471 and if not, and functional alleles were retained, could that suggest a repurposing of the genes
472 for rhythmicity, and its plasticity, to yield adaptation? Further isolation of the causal genes
473 underlying DOC and the study of their possible pleiotropic effects on agronomic traits, as
474 well their biochemical functions, will be required to answers to these questions.

475

476 **Materials and methods**

477 *Plant material and genotypic data*

478 For this clock thermal plasticity analysis, we used tree Barley panel: wild barley
479 (*Hordeum spontaneum*), interspecific multiparent barley population HEB-25 and breeding
480 cultivated panel (*H. vulgare*). We selected two hundred and eighty-three accessions of wild
481 barley which are single-seed descents from our original Barley1K collection (25). The B1K
482 accessions were collected in hierarchical manner (5 microsites in each location) from 51 sites
483 that represent a broad genetic and ecogeographic adaptation. We initially attempted to select
484 one representative accessions from each micro-site and more from sites showing relatively
485 higher genetic diversity based on SSR analysis of the collection (25). For the HEB
486 population, we selected three hundred thirty-eight lines that represent all 25 families. These
487 25 HEB families were generated by introduction of different *H. spontaneum* accessions into
488 the background of the cultivated Barke background (26). All original BC₁S₃ lines (two
489 generations earlier) and their corresponding parents were genotyped using the barley
490 Infinium iSelect 9K chip (26), consisting of 7864 SNPs (46). The single seed descended HEB-
491 25 lines we used for the clock measurements are a BC₁S_{3::5}. Two hundred thirty-two
492 cultivated barley (*H. vulgare*) from the US Spring Two-Row Multi-Environment Trial
493 (S2MET) are an advanced cultivated breeding material for adapting into environmental
494 changes (27). This panel consists of one-eighty-three lines from five U.S. breeding programs
495 and 50 are from crosses between some of these lines.

496

497 *Clock phenotype under optimal and high temperature*

498 To mimic the natural growth conditions of the wild barley population in the Southern Levant,
499 where the original Barley1K infrastructure was collected (25). Plants were grown to the

500 emergence of the fourth leaf under 10h light and 14h dark, at a constant temperature of 20°C.
501 We grew the two other panels up to the emergence of the fourth leaf under 14h light and 10h
502 dark to mimic the spring growing of Barke in Europe and in the US. Following this
503 entrainment of the plants for four weeks, we moved them to the high-throughput SensyPAM
504 (SensyTIV, Aviel, Israel) custom-designed to allow F measurements in up to 240 plants for
505 each experiment (see details at (8)). For the clock measurement, F was measured every 2.5
506 hours, for 3 days, in continuous light. We measured each genotype twice under each
507 temperature, with 4 to 5 plants included in each round. For the clock analysis, NPQ_{ss} ((F_m-
508 F_{mlss})/F_{mlss}) was calculated and normalized by the one control line that appeared in each
509 experiment. The circadian clock free running period (FRP), amplitude (AMP) and amplitude
510 error were extracted using the BioDare2 website (<https://biodare2.ed.ac.uk>). The input data
511 was set to "cubic dtr" and the "MFourFit" was used as the analysis method (47).

512

513 *Statistical analysis*

514 We used the JMP version 14.0 statistical package (SAS Institute, Cary, NC, USA) for
515 statistical analyses and for generating reaction norms for the means and standard errors of the
516 different traits. Student's t-Tests between treatments were conducted per panel using the 'Fit
517 Y by X' function. A factorial model was employed for the analysis of variance (ANOVA,
518 table Sx), using 'Fit model', with temperature treatment and panel as fixed effects. The
519 density plot was made using MVAPP(48).

520

521 *Genome-wide association study (GWAS)*

522 We conducted genome-wide association to identify trait variations, per-se, under optimal and
523 high temperatures (OT and HT), and to assess di-genic interactions (2D-scan). Since the
524 methods of choice (genetic model and statistics) for the genome scan have a major effect on
525 the loci identified we compared between several options to point into most reliable signals
526 that we could support by more than one method:

527

528 *Extended Bayesian Lasso (EBL)*: EBL (49) is the extension of Bayesian Lasso (50), that
529 separates the regularisation parameter into a shrinkage factor for the overall model sparsity
530 (δ^2) and a shrinkage factor for individual markers (η_p^2). This approach is intended to assign
531 different magnitudes of shrinkage to individual marker effects. In EBL, the following linear
532 model was used:

$$y_i = \sum_{p=1}^P x_{ip} \beta_p + \varepsilon_i$$

533 where y_i is a phenotypic value of individual i , x_{ip} is a genotype of marker p of individual i ,
534 β_p is a effect of marker p , and ε_i is a residual for the individual i with $\varepsilon_i \sim N(0, \sigma_e^2)$. Each
535 regression parameter β_p is assumed to follow

$$\beta_p \sim N\left(0, 1/\tau_0^2 \tau_p^2\right)$$

536 where τ_p^2 determines the magnitude of shrinkage for β_p , and $1/\tau_0^2$ is the residual variance,
537 respectively. Then, τ_p^2 was assumed to follow a prior distribution

$$\tau_p^2 \sim Inv - G\left(1, \delta^2 \eta_p^2 / 2\right)$$

538 where $Inv - G$ indicates the inverse Gamma distribution, δ^2 is the shrinkage factor for all
539 markers and η_p^2 is the shrinkage factor unique to marker p . A prior distribution for δ^2
540 was $\delta^2 \sim G(1, 1)$, and for η_p^2 was $\eta_p^2 \sim G(1, \theta)$ where the rate parameter θ is the
541 hyperparameter for EBL. Three values of θ were tested: 0.1, 1, and 5 and a nested five-fold
542 CV was performed to determine the optimal hyperparameter. The EBL was performed by
543 using function *vigor* in the R package “VIGoR” (51). Then absolute value of β_p was used as
544 the GWAS score.

545
546

547 **Tassel MLM:** Mixed Linear Model (MLM) in Tassel software considers both population
548 structure and kinship in the association analysis. It reduces Type I error due to relatedness and
549 population structure. MLM was used to identify the associations between phenotypic and
550 genotypic data in Tassel v5.2.5.0 (52) with optimal compression and variance component
551 estimation by P3D (population parameters previously determined). The P value indicated the
552 degree of association between a SNP marker and a trait, and the
553 R^2 depicts the variation explained by the significantly associated markers. Markers with an
554 adjusted $-\log_{10}(\text{P-value}) \geq 3.0$ were regarded as significant for all traits.

555

556 **Two-dimensional genome scan (2D-scan)**

557 For 2D-scan, we considered following linear mixed models:

$$M_{full} : y = \mu + g + \beta_i m_i + \beta_j m_j + \gamma_{ij} (m_i \times m_j) + \epsilon$$

$$M_{add} : y = \mu + g + \beta_i m_i + \beta_j m_j + \epsilon$$

$$M_i : y = \mu + g + \beta_i m_i + \epsilon$$

$$M_j : y = \mu + g + \beta_j m_j + \epsilon$$

558 where y represents a vector of phenotype, m_x represents coded genotypic values of marker
559 x (-1 and 1 for homozygous, 0 for heterozygous), β_x represents effect of marker x , γ_{ij}
560 represents a vector of coefficients for interaction between marker i and j ($m_i \times m_j$), The variable
561 g models the genetic background of each line as a random effect with $g \sim N(0, K\sigma_G^2)$, where K
562 is a kinship matrix calculated from the nucleotide polymorphisms, and σ_G^2 is the genetic
563 variance. ϵ represents the residual error such that $\epsilon \sim N(0, I\sigma_e^2)$, where I is an identity matrix
564 and σ_e^2 is the residual variance. M_i and M_j are equivalent to the model used for single marker
565 based GWAS. M_{add} is a model to test additive effects of two loci while M_{full} include both
566 additive and interactive effects of two loci. Then, we derived two P -values from the above
567 models.

$$LL_1 = \max\{LL_i, LL_j\}$$

$$P_{add} = \chi_1^2(LL_{add} - LL_1)$$

$$P_{int} = \chi_{df.int}^2(LL_{int} - LL_{add})$$

568 where LL_{int} , LL_{add} , LL_i and LL_j are log likelihood for M_{int} , M_{add} , M_i and M_j , respectively. P_{add}
569 was used to test significance of addition of a locus to the another. P_{int} was used to test
570 significance of interactive effect. $df.int$ is degree of freedom for two loci interactive effect
571 that is equivalent to number of combination patterns in the given two loci. To solve the linear
572 mixed models used in the 2D-scan, we used the R package “gaston” (53)(54). Maximum
573 likelihood estimates of variance components were obtained using function *lmm.diago*, and
574 log likelihood of each model was calculated using function *lmm.diago.profile.likelihood*.

575

576 *Correlations between environmental covariates and GWAS results*

577 The full environmental covariate data appears at Neyhart et al. (27). For the analysis in our
578 current study we calculated the daily mean temperature according to the daily min and max
579 temperature in each field trial. From this data we calculated the mean of the minimal (min),
580 maximal(max) and mean daily temperature, and the range of the mean daily temperature. In
581 addition, we calculated the maximum of the mean and max temperatures and the CV for the
582 min, max and mean daily temperature. We also used the cumulative perception in each trial
583 and calculate the GDD. We also normalized the HEA and GY in each trial following similar
584 normalization conducted by Merchuk et al. (2018) for multiple year

$$\frac{HEA_{line} - \min HEA_{trial}}{\max HEA_{trial} - \min HEA_{trial}}$$

585

586

587

588 **ACKNOWLEDGEMENTS**

589 This work was supported by the Israeli Science Foundation (ISF) program (1270/17) and the

590 Chief Scientist Competitive Grant (20-01-0080) from the Ministry of Agriculture to E.F.

591

592

593 **Bibliography**

594

595 1. C. R. McClung, Plant circadian rhythms. *Plant Cell* (2006)

596 <https://doi.org/10.1105/tpc.106.040980>.

597 2. A. N. Dodd, *et al.*, Cell biology: Plant circadian clocks increase photosynthesis,
598 growth, survival, and competitive advantage. *Science* (80-.). (2005)

599 <https://doi.org/10.1126/science.1115581>.

600 3. K. Greenham, C. R. McClung, Integrating circadian dynamics with physiological
601 processes in plants. *Nat. Rev. Genet.* (2015) <https://doi.org/10.1038/nrg3976>.

602 4. K. D. Edwards, J. R. Lynn, P. Gyula, F. Nagy, A. J. Millar, Natural allelic variation in
603 the temperature-compensation mechanisms of the *Arabidopsis thaliana* circadian
604 clock. *Genetics* (2005) <https://doi.org/10.1534/genetics.104.035238>.

605 5. W. Y. Kim, *et al.*, ZEITLUPE is a circadian photoreceptor stabilized by GIGANTEA
606 in blue light. *Nature* (2007) <https://doi.org/10.1038/nature06132>.

607 6. M. K. Choudhary, Y. Nomura, L. Wang, H. Nakagami, D. E. Somers, Quantitative
608 circadian phosphoproteomic analysis of *Arabidopsis* reveals extensive clock control of
609 key components in physiological, metabolic, and signaling pathways. *Mol. Cell.*
610 *Proteomics* (2015) <https://doi.org/10.1074/mcp.M114.047183>.

611 7. Y. Dakhiya, D. Hussien, E. Fridman, M. Kiflawi, R. Green, Correlations between
612 circadian rhythms and growth in challenging environments. *Plant Physiol.* (2017)
613 <https://doi.org/10.1104/pp.17.00057>.

614 8. E. Bdolach, *et al.*, Thermal plasticity of the circadian clock is under nuclear and
615 cytoplasmic control in wild barley. *Plant Cell Environ.* (2019)
616 <https://doi.org/10.1111/pce.13606>.

617 9. P. D. Gould, *et al.*, Delayed fluorescence as a universal tool for the measurement of
618 circadian rhythms in higher plants. *Plant J.* (2009) [https://doi.org/10.1111/j.1365-](https://doi.org/10.1111/j.1365-313X.2009.03819.x)
619 [313X.2009.03819.x](https://doi.org/10.1111/j.1365-313X.2009.03819.x).

620 10. L. Valleliau-Bindschedler, E. Mösinger, J. P. Métraux, P. Schweizer, Structure,
621 expression and localization of a germin-like protein in barley (*Hordeum vulgare* L.)
622 that is insolubilized in stressed leaves. *Plant Mol. Biol.* (1998)
623 <https://doi.org/10.1023/A:1005982715972>.

624 11. M. Martínez, I. Rubio-Somoza, P. Carbonero, I. Díaz, A cathepsin B-like cysteine
625 protease gene from *Hordeum vulgare* (gene CatB) induced by GA in aleurone cells is
626 under circadian control in leaves. *J. Exp. Bot.* (2003)

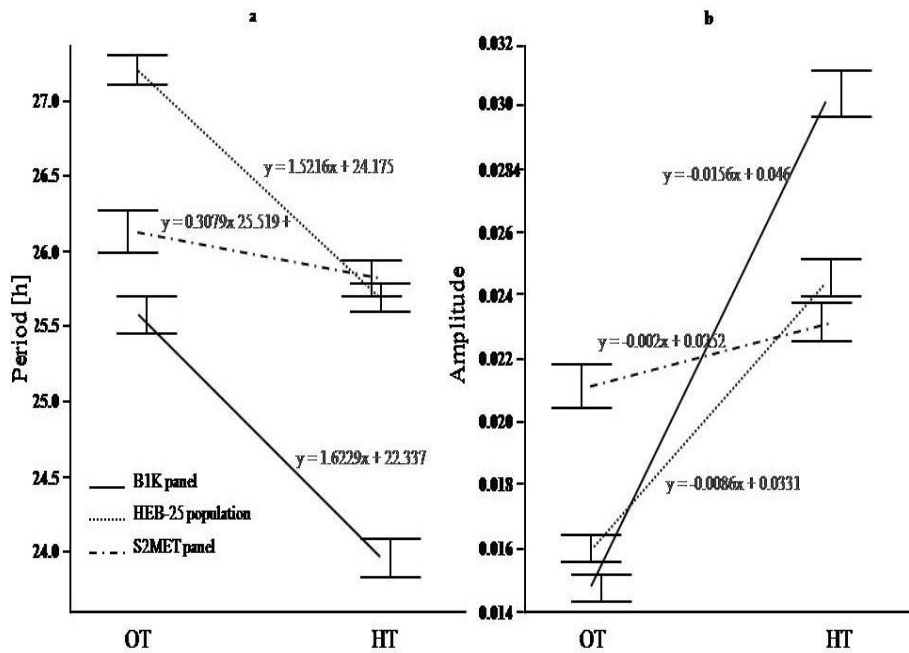
- 627 <https://doi.org/10.1093/jxb/erg099>.
- 628 12. C. Lillo, Circadian rhythmicity of nitrate reductase activity in barley leaves. *Physiol.*
629 *Plant.* (1984) <https://doi.org/10.1111/j.1399-3054.1984.tb05900.x>.
- 630 13. S. Nagasaka, *et al.*, Time course analysis of gene expression over 24 hours in Fe-
631 deficient barley roots. *Plant Mol. Biol.* (2009) [https://doi.org/10.1007/s11103-008-](https://doi.org/10.1007/s11103-008-9443-0)
632 9443-0.
- 633 14. R. P. Dunford, S. Griffiths, V. Christodoulou, D. A. Laurie, Characterisation of a
634 barley (*Hordeum vulgare* L.) homologue of the Arabidopsis flowering time regulator
635 GIGANTEA. *Theor. Appl. Genet.* (2005) <https://doi.org/10.1007/s00122-004-1912-5>.
- 636 15. A. Turner, J. Beales, S. Faure, R. P. Dunford, D. A. Laurie, Botany: The pseudo-
637 response regulator Ppd-H1 provides adaptation to photoperiod in barley. *Science* (80-
638). (2005) <https://doi.org/10.1126/science.1117619>.
- 639 16. J. A. Higgins, P. C. Bailey, D. A. Laurie, Comparative genomics of flowering time
640 pathways using brachypodium distachyon as a model for the temperate Grasses. *PLoS*
641 *One* (2010) <https://doi.org/10.1371/journal.pone.0010065>.
- 642 17. C. Campoli, M. Shtaya, S. J. Davis, M. von Korff, Expression conservation within the
643 circadian clock of a monocot: natural variation at barley Ppd-H1 affects circadian
644 expression of flowering time genes, but not clock orthologs. *BMC Plant Biol.* (2012)
645 <https://doi.org/10.1186/1471-2229-12-97>.
- 646 18. C. Campoli, *et al.*, HvLUX1 is a candidate gene underlying the early maturity 10 locus
647 in barley: Phylogeny, diversity, and interactions with the circadian clock and
648 photoperiodic pathways. *New Phytol.* (2013) <https://doi.org/10.1111/nph.12346>.
- 649 19. S. Faure, *et al.*, Mutation at the circadian clock gene EARLY MATURITY 8 adapts
650 domesticated barley (*Hordeum vulgare*) to short growing seasons. *Proc. Natl. Acad.*
651 *Sci. U. S. A.* (2012) <https://doi.org/10.1073/pnas.1120496109>.
- 652 20. S. Zakhrabekova, *et al.*, Induced mutations in circadian clock regulator Mat-a
653 facilitated short-season adaptation and range extension in cultivated barley. *Proc. Natl.*
654 *Acad. Sci. U. S. A.* (2012) <https://doi.org/10.1073/pnas.1113009109>.
- 655 21. L. Müller, *et al.*, Differential effects of day-night cues and the circadian clock on the
656 barley transcriptome. *Plant Physiol.* (2020) <https://doi.org/10.1104/pp.19.01411>.
- 657 22. C. Bendix, C. M. Marshall, F. G. Harmon, Circadian Clock Genes Universally Control
658 Key Agricultural Traits. *Mol. Plant***8**, 1135–1152 (2015).
- 659 23. R. L. Murphy, *et al.*, Coincident light and clock regulation of pseudoreponse regulator
660 protein 37 (PRR37) controls photoperiodic flowering in sorghum. *Proc. Natl. Acad.*

- 661 *Sci. U. S. A.* (2011) <https://doi.org/10.1073/pnas.1106212108>.
- 662 24. N. A. Müller, L. Zhang, M. Koornneef, J. M. Jiménez-Gómez, Mutations in EID1 and
663 LNK2 caused light-conditional clock deceleration during tomato domestication. *Proc.*
664 *Natl. Acad. Sci. U. S. A.* (2018) <https://doi.org/10.1073/pnas.1801862115>.
- 665 25. S. Hübner, *et al.*, Strong correlation of wild barley (*Hordeum spontaneum*) population
666 structure with temperature and precipitation variation. *Mol. Ecol.* (2009)
667 <https://doi.org/10.1111/j.1365-294X.2009.04106.x>.
- 668 26. A. Maurer, *et al.*, Modelling the genetic architecture of flowering time control in
669 barley through nested association mapping. *BMC Genomics* (2015)
670 <https://doi.org/10.1186/s12864-015-1459-7>.
- 671 27. J. L. Neyhart, *et al.*, Registration of the S2MET Barley Mapping Population for Multi-
672 Environment Genomewide Selection. *J. Plant Regist.* (2019)
673 <https://doi.org/10.3198/jpr2018.06.0037crmp>.
- 674 28. N. A. Müller, *et al.*, Domestication selected for deceleration of the circadian clock in
675 cultivated tomato. *Nat. Genet.* (2015) <https://doi.org/10.1038/ng.3447>.
- 676 29. L. Merchuk-Ovnat, *et al.*, Genome scan identifies flowering-independent effects of
677 barley HsDry2.2 locus on yield traits under water deficit. *J. Exp. Bot.* (2018)
678 <https://doi.org/10.1093/jxb/ery016>.
- 679 30. E. B. Josephs, Determining the evolutionary forces shaping $G \times E$. *New Phytol.* (2018)
680 <https://doi.org/10.1111/nph.15103>.
- 681 31. Y. Shavrukov, *et al.*, Early flowering as a drought escape mechanism in plants: How
682 can it aid wheat production? *Front. Plant Sci.* (2017)
683 <https://doi.org/10.3389/fpls.2017.01950>.
- 684 32. K. M. Olsen, J. F. Wendel, A Bountiful Harvest: Genomic Insights into Crop
685 Domestication Phenotypes. *Annu. Rev. Plant Biol.* (2013)
686 <https://doi.org/10.1146/annurev-arplant-050312-120048>.
- 687 33. A. L. Caicedo, *et al.*, Genome-wide patterns of nucleotide polymorphism in
688 domesticated rice. *PLoS Genet.* (2007) <https://doi.org/10.1371/journal.pgen.0030163>.
- 689 34. S. I. Wright, *et al.*, Evolution: The effects of artificial selection on the maize genome.
690 *Science (80-.)*. (2005) <https://doi.org/10.1126/science.1107891>.
- 691 35. S. Tanksley, S. McCouch, Seed banks and molecular maps: unlocking genetic
692 potential from the wild. *Science (80-.)*. **277**, 1063–1066 (1997).
- 693 36. H. Bourguiba, *et al.*, Loss of genetic diversity as a signature of apricot domestication
694 and diffusion into the Mediterranean Basin. *BMC Plant Biol.* **12**, 49 (2012).

- 695 37. J. Shi, J. Lai, Patterns of genomic changes with crop domestication and breeding.
696 *Curr. Opin. Plant Biol.* (2015) <https://doi.org/10.1016/j.pbi.2015.01.008>.
- 697 38. A. Pankin, J. Altmüller, C. Becker, M. von Korff, Targeted resequencing reveals
698 genomic signatures of barley domestication. *New Phytol.* (2018)
699 <https://doi.org/10.1111/nph.15077>.
- 700 39. M. A. Jones, Retrograde signalling as an informant of circadian timing. *New Phytol.*,
701 1–5 (2018).
- 702 40. E. Fridman, M. R. Prusty, A. Faigenboim-Doron, E. Bdolach, Barley Cytoplasmic
703 Multi Parent Population (CMPP) for Studying Evolution of Plasticity Under
704 Domestication in *The Allied Genetics Conference*, (Genetics Society of America,
705 2020).
- 706 41. S. M. Wadgyamar, *et al.*, Identifying targets and agents of selection: innovative
707 methods to evaluate the processes that contribute to local adaptation. *Methods Ecol.*
708 *Evol.* (2017) <https://doi.org/10.1111/2041-210X.12777>.
- 709 42. O. Savolainen, M. Lascoux, J. Merilä, Ecological genomics of local adaptation. *Nat.*
710 *Rev. Genet.* (2013) <https://doi.org/10.1038/nrg3522>.
- 711 43. D. B. Lowry, *et al.*, QTL × environment interactions underlie adaptive divergence in
712 switchgrass across a large latitudinal gradient. *Proc. Natl. Acad. Sci. U. S. A.* (2019)
713 <https://doi.org/10.1073/pnas.1821543116>.
- 714 44. S. O. Assanga, *et al.*, Mapping of quantitative trait loci for grain yield and its
715 components in a US popular winter wheat TAM 111 using 90K SNPs. *PLoS One*
716 (2017) <https://doi.org/10.1371/journal.pone.0189669>.
- 717 45. A. Börner, G. H. Buck-Sorlin, P. M. Hayes, S. Malyshev, V. Korzun, Molecular
718 mapping of major genes and quantitative trait loci determining flowering time in
719 response to photoperiod in barley. *Plant Breed.* (2002) <https://doi.org/10.1046/j.1439-0523.2002.00691.x>.
- 720
- 721 46. J. Comadran, *et al.*, Natural variation in a homolog of Antirrhinum
722 CENTRORADIALIS contributed to spring growth habit and environmental adaptation
723 in cultivated barley. *Nat. Genet.* **44**, 1388–92 (2012).
- 724 47. T. Zielinski, A. M. Moore, E. Troup, K. J. Halliday, A. J. Millar, Strengths and
725 limitations of period estimation methods for circadian data. *PLoS One* (2014)
726 <https://doi.org/10.1371/journal.pone.0096462>.
- 727 48. M. M. Julkowska, S. Saade, G. Agarwal, G. Gao, Y. Pailles, MVApp — Multivariate
728 Analysis Application for Streamlined Data Analysis and Curation 1 [OPEN]. **180**,

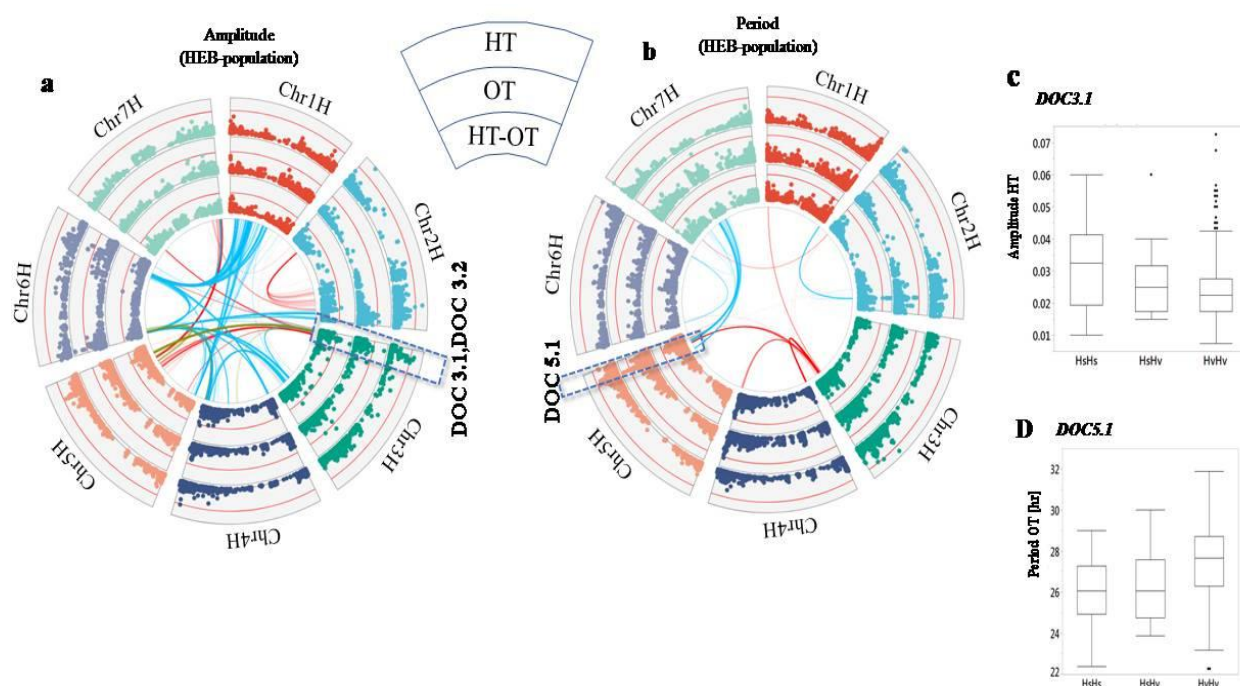
- 729 1261–1276 (2019).
- 730 49. C. M. Mutshinda, M. J. Sillanpää, Extended Bayesian LASSO for multiple quantitative
731 trait loci mapping and unobserved phenotype prediction. *Genetics* (2010)
732 <https://doi.org/10.1534/genetics.110.119586>.
- 733 50. T. Park, G. Casella, The Bayesian Lasso. *J. Am. Stat. Assoc.* (2008)
734 <https://doi.org/10.1198/016214508000000337>.
- 735 51. , VIGoR: Variational Bayesian Inference for Genome-Wide Regression. *J. Open Res.*
736 *Softw.* (2016) <https://doi.org/10.5334/jors.80>.
- 737 52. P. J. Bradbury, *et al.*, TASSEL: Software for association mapping of complex traits in
738 diverse samples. *Bioinformatics* (2007) <https://doi.org/10.1093/bioinformatics/btm308>.
- 739 53. C. Xhaard, *et al.*, Heritability of a resting heart rate in a 20-year follow-up family
740 cohort with GWAS data: Insights from the STANISLAS cohort. *Eur. J. Prev. Cardiol.*
741 (2019) <https://doi.org/10.1177/2047487319890763>.
- 742 54. H. Perdry, C. Dandine-Roulland, gaston: Genetic Data Handling (QC, GRM, LD,
743 PCA) & Linear Mixed Models.
744
745
746
747
748
749
750
751
752
753
754
755
756
757
758
759
760
761
762

763 Figures legends



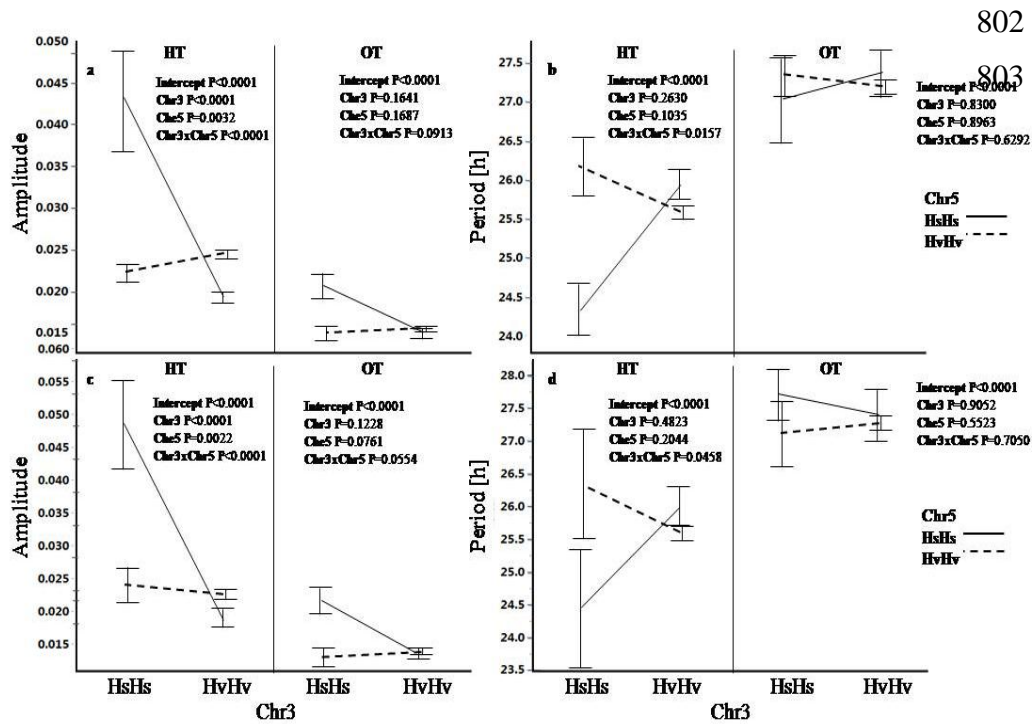
764 **Figure 1:** Differential rhythms and thermal plasticity between barley wild panel (Barley1K,
765 B1K), interspecific multiparent population (HEB) and cultivated breeding (S2MET) plant
766 material. Circadian rhythms reaction norms of barley wild *H. spontaneum* panel (n=283),
767 HEB-25 interspecific multiparent population (N=338) and advanced cultivated *H. vulgare*
768 breeding material (N=232) under two thermal environments, optimal temperature (OT; 22°C)
769 and high temperature (HT; 32°C) for clock period (A) and amplitude (B).

770
771
772
773
774
775
776
777
778
779
780
781
782



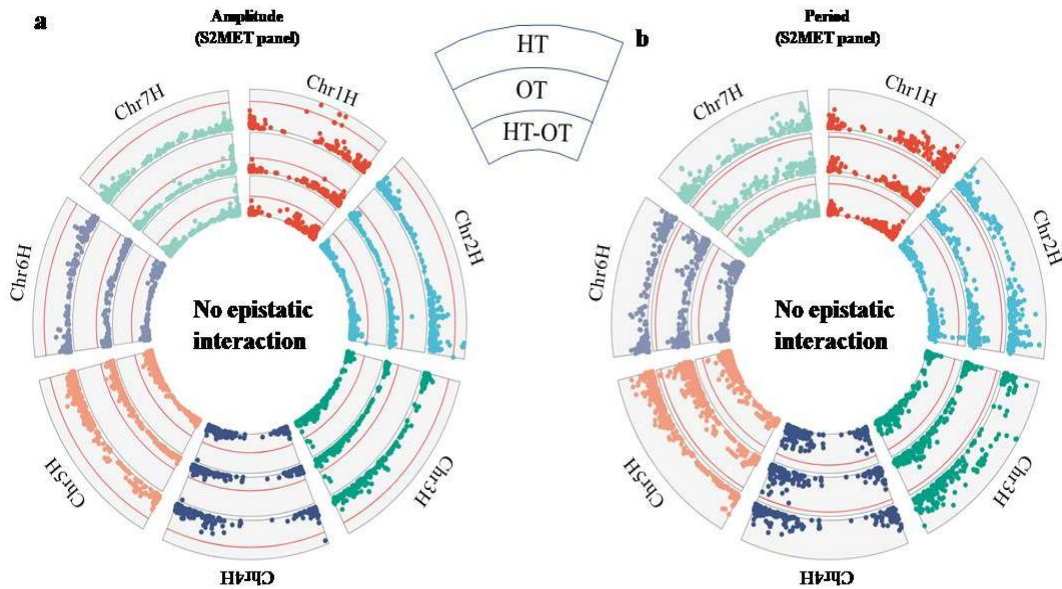
783 **Figure 2:** Circos plots depicting the GWAS results for (a)Amplitude and (b)Period of the
 784 clock in HEB population. Barley chromosomes in the plot are depicted in different
 785 colors. Outer, middle and inner Manhattan plots indicate $-\log_{10}(p)$ of one-dimensional GWAS
 786 for high temperature (HT), optimal temperature (OT) and for the delta (HT-OT), respectively.
 787 Red lines in the Manhattan plots indicate significant threshold ($p = 0.001$). Links in the center
 788 of the circles indicate significant di-genic interactions detected by two-dimensional two-locus
 789 genome-wide association study ($p = 0.001$). Red, blue and yellow links indicate high
 790 temperature, optimal temperature and the delta, respectively. *DOC3.1*, *3.2*&*5.1* appear in all
 791 the three methods (LMM,MLM and EBL) analysis and hence are demarked in the circos.
 792 Boxplots of clock plasticity for (c) *DOC3.1* effects on Amplitude and (d) *DOC5.1* effects on
 793 Period. HsHs, homozygous for wild allele; HsHv, heterozygous for wild and cultivated allele,
 794 and HvHv, homozygous for cultivated allele.

795
 796
 797
 798
 799
 800
 801



804 **Figure 3:** Epistatic interactions between DOC loci on chromosome 3 and 5 for clock
 805 amplitude and period. Least-square mean value comparisons (reaction norms) for the (a and b)
 806 *DOC3.1* (position 30,927,745) and (c and d) *DOC3.2* (position 47,570,630) genotypes under
 807 optimal temperature (OT; 22°C) and high temperature (HT; 32°C) in the HEB population. A
 808 two-way ANOVA including each pair of loci in chromosome 3 and 5 tested if the interaction
 809 is significant.

810
 811
 812
 813
 814
 815
 816
 817
 818
 819
 820
 821
 822
 823



824

825 **Figure 4:** Circos plots depicting the GWAS results for (a) Amplitude and (b) Period in
826 S2MET panel. Barley chromosomes in the plot are depicted in different colors. Outer, middle
827 and inner Manhattan plots indicate $-\log_{10}(p)$ of one-dimensional GWAS for high temperature
828 (HT), optimal temperature (OT) and the delta between values (HT-OT), respectively. Red
829 lines in the Manhattan plots indicate significant threshold ($p = 0.001$).

830

831

832

833

834

835

836

837

838

839

840

841

842

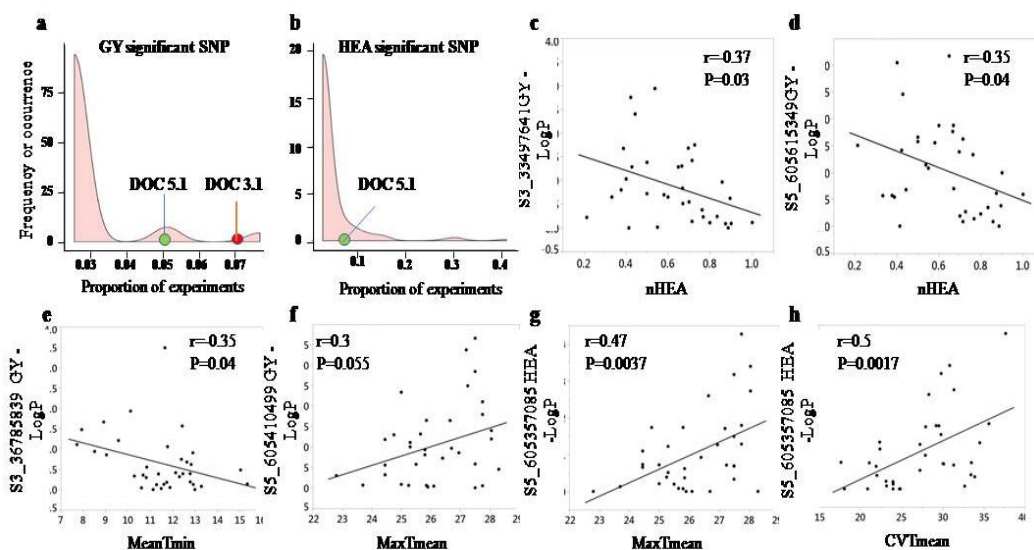
843

844

845

846

847

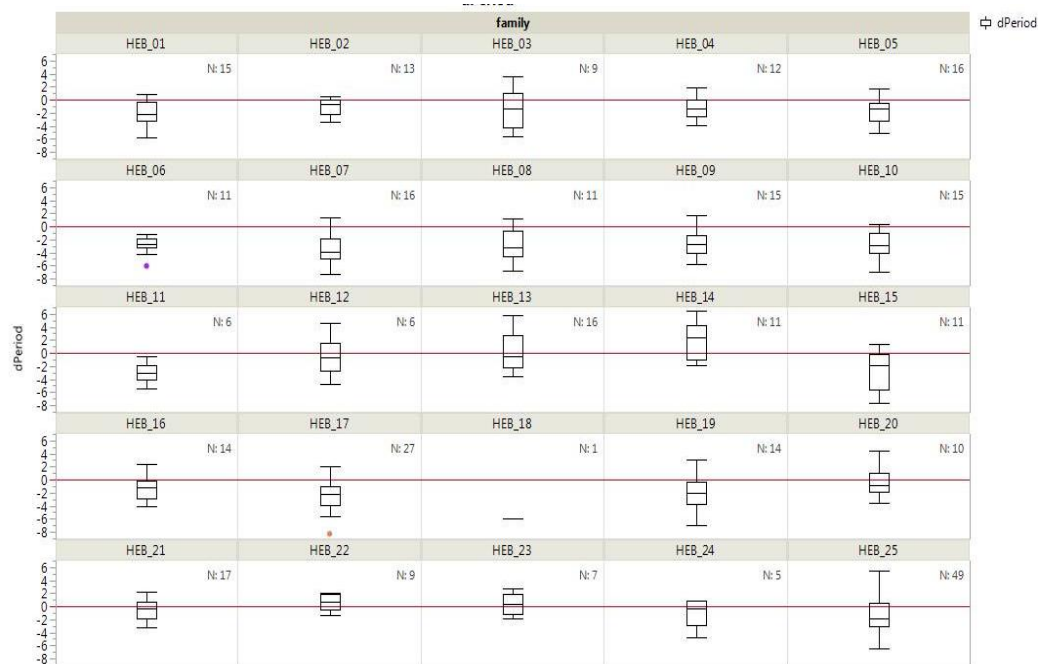


849 **Figure 5:** QTL-environment association for DOC loci show their stable and temperature-
 850 dependent effects on heading date (HEA) and grain yield (GY) variation in S2MET panel
 851 grown across US. Density plots representing the frequency SNP that are significantly
 852 ($LOD > 3$) associated with (a) HEA or (b) GY variation. Frequency or occurrence (X-axis) is
 853 expressed as proportion of experiments (out of 39) in which association marker-traits is
 854 significant. Red and green dots on the X-axis demarcate the occurrence of *DOC3.1* and
 855 *DOC5.1* loci for GY and HEA. The correlations between normalized heading date at
 856 experimental site and significance of the (c) *DOC3.1* or (d) *DOC5.1* association with GY in
 857 the S2MET panel. The correlations between Tmin in experimental sites and GWAS $-\log_{10}(p)$
 858 values for (e) *DOC3.1* and (f) *DOC5.1* for GY. *DOC5.1*-temperature association is depicted
 859 by the positive correlations of (g) minimal temperature (Tmin) and (h) CV of Tmin with
 860 GWAS $-\log_{10}(p)$ values for *DOC5.1* effect on GY in S2MET panel.

861

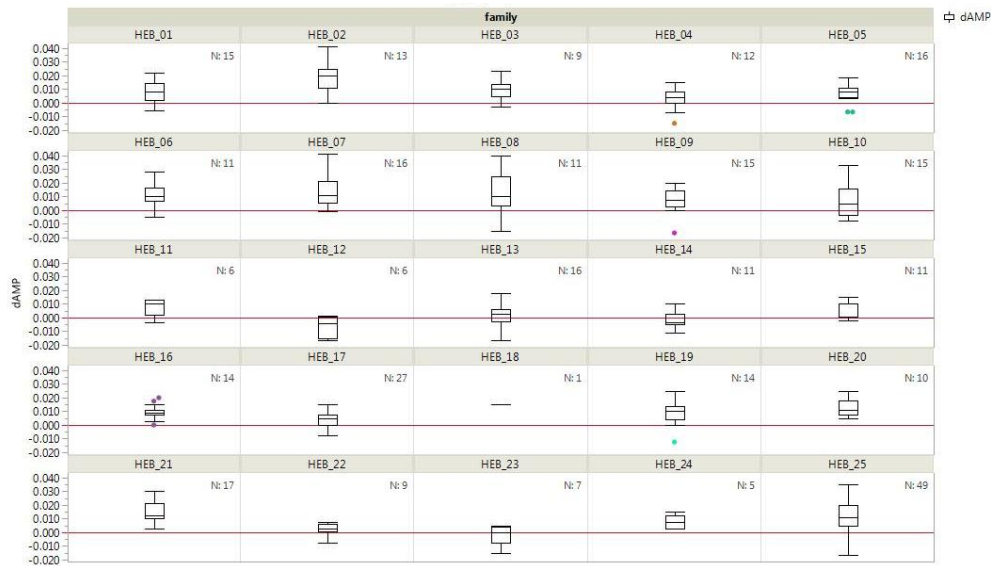
862

863 Supplementary figures legends



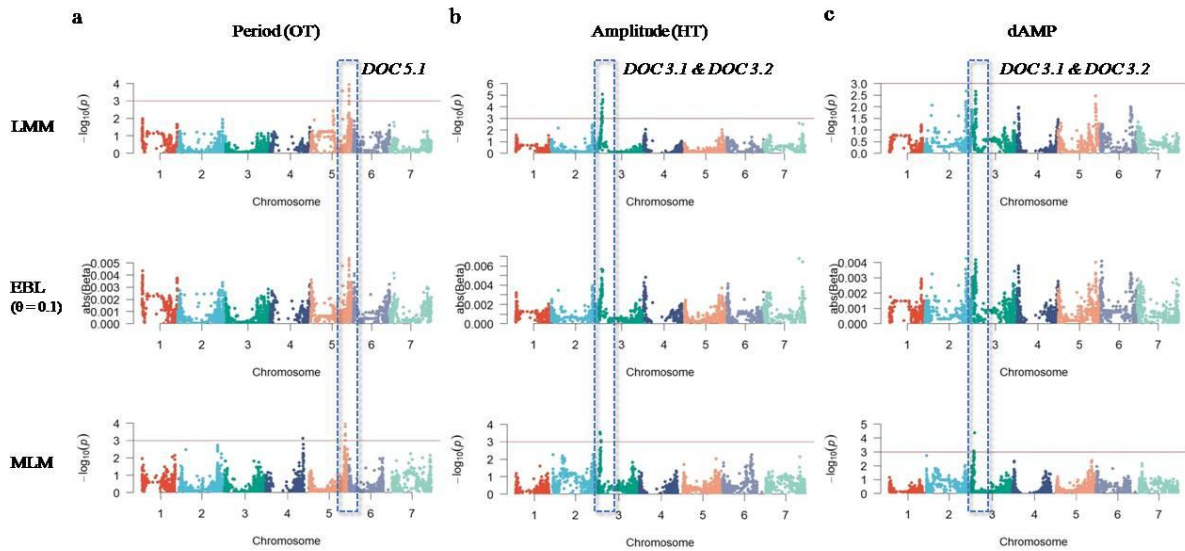
864 **Figure S1:**Differential period thermal plasticity in the HEB-25 families. Box plots for
865 dPeriod among each of the sub-populations (each with a different *H. spontaneum* donor;
866 (26)) of the interspecific multi-parent barley population HEB-25. dPeriod is the period under
867 high temperature (HT; 32°C) minus that under optimal temperature (OT; 22°C). The red line
868 represents dPeriod=0 that means no period plasticity.

869
870
871
872
873
874
875
876
877
878
879
880
881
882



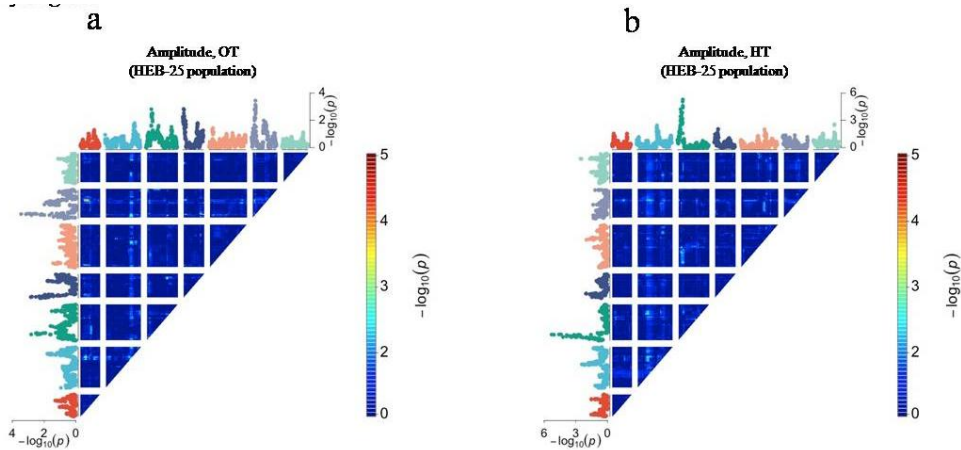
883 **Figure S2:**Differential amplitude thermal plasticity in the HEB-25 families. Box plots for
884 dAmplitude among each of the sub-populations (each with a different *H. spontaneum* donor;
885 (26)) of the interspecific multiparent barley population HEB-25. dPAmpplitude is the
886 amplitude under high temperature (HT; 32°C) minus that under optimal temperature (OT;
887 22°C). The red line represents dPAmpitude=0 that means no amplitude plasticity.

888
889
890
891
892
893
894
895
896
897
898
899
900
901
902
903
904
905
906



907 **Figure S3:** Significant DOCs detected in more than one method (LMM,EBL and MLM) of
908 the GWAS analysis.(a) *DOC5.1* identified for period OT (b) *DOC3.1* and *3.2* identified for
909 amplitude HT and (c) *DOC3.1* and *3.2* identified for delta amplitude.

910
911
912
913
914
915
916
917
918
919
920
921
922
923
924
925
926
927
928
929



930

931 **Figure S4:**Genome-wide scan for amplitude in HEB-25 population under (a) optimal
932 temperature (OT) and (b) high temperature (HT).Heat map for two-dimensional genome scan
933 with a two-loci interaction model. The Manhattan plots on x- and y-axes in each panel
934 indicate result of one-locus model genome scan. Genome scans were performed using linear
935 mixed model that account population structure as the covariates.

936

937

938

939

940

941

942

943

944

945

946

947

948

949

950

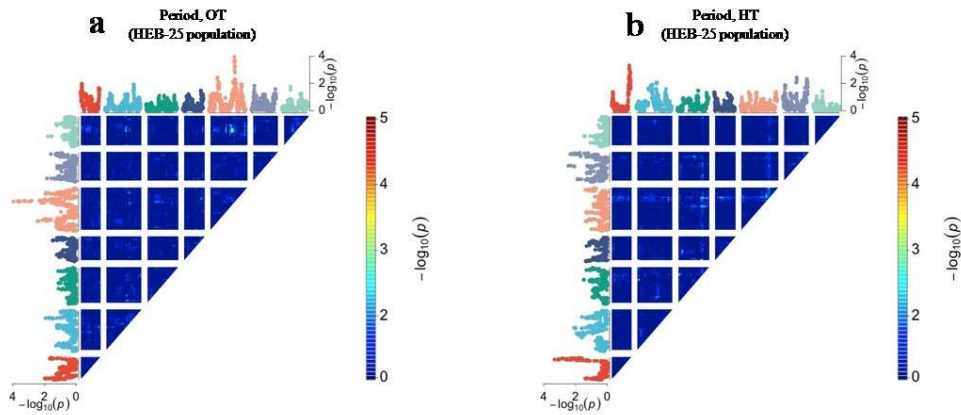
951

952

953

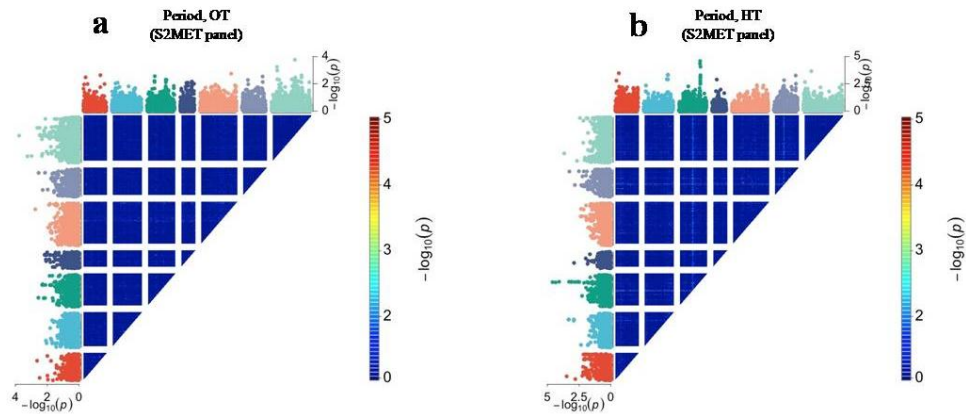
954

955



956 **Figure S5:** Genome-wide scan for period in HEB-25 population under (a) optimal
957 temperature (OT) and (b) high temperature (HT). Heat map for two-dimensional genome scan
958 with a two-loci interaction model. The Manhattan plots on x- and y-axes in each panel
959 indicate result of one-locus model genome scan. Genome scans were performed using linear
960 mixed model that account population structure as the covariates.

961
962
963
964
965
966
967
968
969
970
971
972
973
974
975
976
977
978
979
980
981



982 **Figure S6:** Genome-wide scan for amplitude in S2MET population under (a) optimal
983 temperature (OT) and (b) high temperature (HT). Heat map for two-dimensional genome scan
984 with a two-loci interaction model. The Manhattan plots on x- and y-axes in each panel
985 indicate result of one-locus model genome scan. Genome scans were performed using linear
986 mixed model that account population structure as the covariates.

987

988

989

990

991

992

993

994

995

996

997

998

999

1000

1001

1002

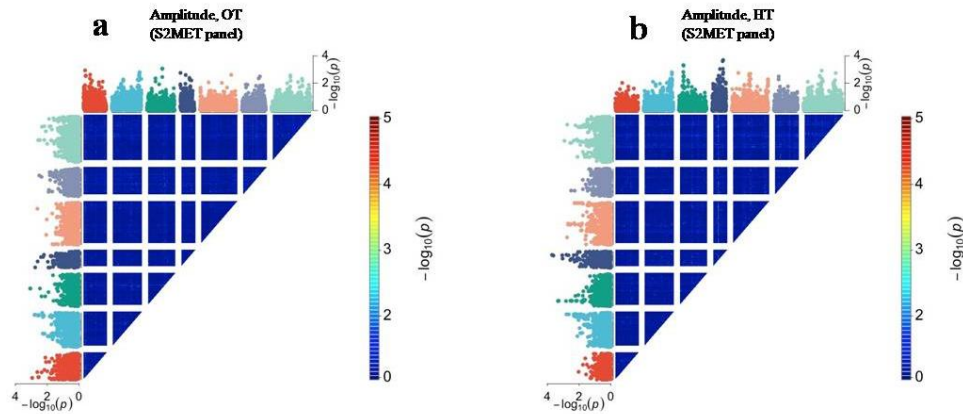
1003

1004

1005

1006

1007



1008 **Figure S7:** Genome-wide scan for period in S2MET population under (a) optimal
1009 temperature (OT) and (b) high temperature (HT). Heat map for two-dimensional genome scan
1010 with a two-loci interaction model. The Manhattan plots on x- and y-axes in each panel
1011 indicate result of one-locus model genome scan. Genome scans were performed using linear
1012 mixed model that account population structure as the covariates.
1013